Springer

KSME

Journal of Mechanical Science and Technology 24 (9) (2010) 1763~1769
www.springerlink.com/content/1738-494x
DOI 10.1007/s12206-010-0604-0

Analysis of total harmonic distortion in microspeakers considering coupling effect †

Lee Chang-Min, Kwon Joong-Hak and Hwang Sang-Moon*

School of Mechanical Engineering, Pusan National University, Busan, 609-735, Korea

(Manuscript Received July 8, 2009; Revised April 29, 2010; Accepted May 24, 2010)

Abstract

With the advent of the mobile phone, Digital Multimedia Broadcasting (DMB) service for multimedia data communication will soon be realized. With regard to the acoustic aspects of this service, a smaller and lighter microspeaker also soon will be implemented in MP3 song players and speakerphones. The sound quality of such microspeakers, as evaluated with reference to total harmonic distortion (THD) is becoming more important. THD is the proportion of the higher-order frequency output response to a sinusoidal input signal. It is affected by uneven magnetic distribution and nonlinear responses of diaphragms. In this work, THD was analyzed in consideration of the coupling effects between mechanical vibration and electromagnetic exciting forces. Simulated THD results were compared with the experimental data. The THD in the lower frequency range increased due to the increased displacement of the voice coil and the elevated high-order component response of the sound pressure.

Keywords: Coupling effect; Microspeaker; Speedance; Sound pressure level (SPL); Total harmonic distortion (THD)

1. Introduction

With the ever-increasing interest in microspeaker sound quality, research on total harmonic distortion (THD) has proceeded apace. THD is a phenomenon corresponding to the linearity of AC signals in electric and electronic circuits, and represents the proportion of high-order components generated when a sinusoidal signal is inputted. It is represented, in microspeakers, as a function of sound pressure. In the previous research, the uneven magnetic field has been analyzed along the voice coil, and the magnetic distortion has been found with reference to the spectra of the flux linkage [1, 2].

However, this approach predicts the tendency of THD only by evaluating the degree of unevenness, without considering the coupling effects of the electromagnetic and mechanical systems. Therefore, it cannot predict quantified THD or changes dependent on frequency characteristics. To find an exact solution, the coupling effects of magnetic distribution and mechanical displacement need to be considered. Indeed, Many coupling analyses have been conducted on electromagnetic mechanical parts such as microspeakers and motors. [3]

In the typical coupling analyses of microspeakers, changes in the magnetic flux density according to the voice coil position have not been considered, and the electric current, magnetic force and vibration displacement have been assumed as sinusoidal. [4] Also, in voltage equations, the back electromotive force and electric current waveform have been calculated only by considering the amplitude, without taking into account the phase. Moreover, mechanical analyses have not considered the distributed forces of the diaphragm surface caused by the back volume of a microspeaker, thus the effects of the amplitude and shape of the back volume were not taken into consideration. This approach cannot be regarded as a complete coupling analysis of a microspeaker, as high-order components cannot be obtained by this means. A past study on motors presented a method to analyze the coupling effects between electromagnetic and mechanical systems. [5] This method obtained the electric current solution by converting the parameters related to the voltage equation to the functions for position, and the torque ripple was obtained using the electric current solution. When the electric current solution was obtained by the voltage equation, however, the motor rotation speed was supposed to be constant. This protocol, however, cannot predict exact mechanical response results. In the case of a motor, it vibrates while rotating in a specific direction and therefore there is no such problem even when the angular velocity is constant.

But the same cannot be said for microspeakers. Accordingly, it is necessary to conduct a more detailed coupling analysis in order to examine the THD of microspeakers. This paper presents a new coupling analysis method to resolve the above-

† This paper was recommended for publication in revised form by Associate Editor Yeon June Kang
* Corresponding author. Tel.: +82 51 510 3204, Fax: +82 51 582 3104
E-mail address: shwang@pusan.ac.kr

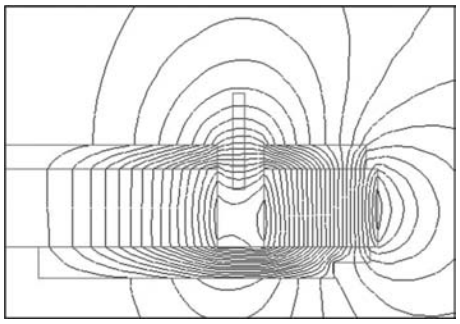

Fig. 1. Microspeaker operating principle.

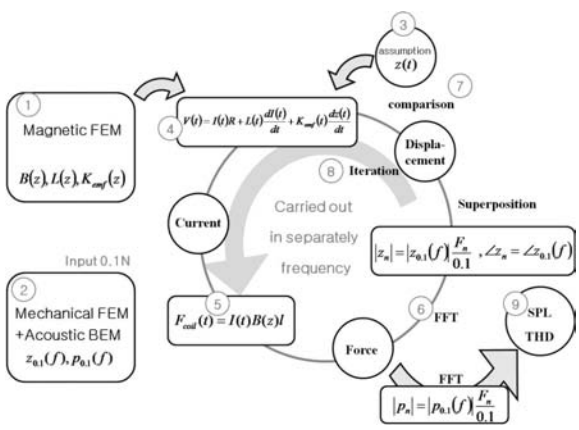

Fig. 2. Flow chart of coupling analysis.

listed problems. The method was verified through experiments, and the experimental data was compared with simulated THD results.

2. Finite element analysis

2.1 Operating principle

Fig. 1 is a schematic of the microspeaker's operating principle. In general, the microspeaker structure as it relates specifically to the electromagnetic and mechanical systems, is similar to that of loud speakers. When electric current flows in the voice coil, electromagnetic force is generated by Fleming's left hand rule. This force excites the voice coil on the diaphragm, which causes the diaphragm to vibrate, which in turn produces the sound.

2.2 Outline of coupling analysis

Fig. 2 shows a flow chart of the coupling analysis treated in this paper. Preparatorily, electromagnetic and mechanical analyses are performed. In the electromagnetic analysis, the magnetic flux density, inductance and speedance are expressed, using FEM, as voice coil displacement functions. In the mechanical analysis, the response displacement of the voice coil and the sound pressure response at the detection position, for a voluntary exciting force of 0.1N, are expressed as frequency functions. Coupling analyses are conducted for each frequency. First, the initial displacement waveform is

Table 1. Material properties of magnetic circuit.

Air	Permeability	$4\pi \times 10^{-7}$ [h/m]
Permanent magnet	Residual flux density	1.3 [T]
	Coercive force	1000 [kA/m]
Yoke	Permeability	See Fig. 4
Top plate		
Voice coil	Permeability	$4\pi \times 10^{-7}$ [h/m]
	Resistance	7.5 [ohm]
	Turns	40

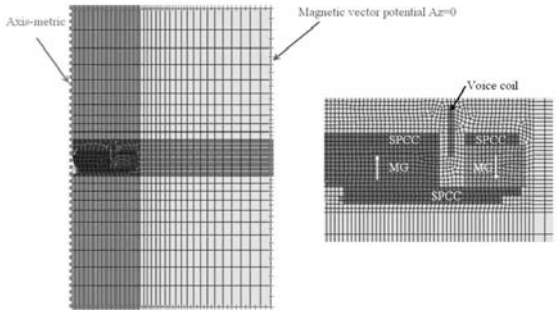

Fig. 3. Boundary condition of magnetic analysis.

assumed using the displacement obtained in the mechanical analysis. Once the displacement waveform is assumed, the magnetic flux density, inductance and speedance obtained through the electromagnetic analysis can be converted into time functions. Accordingly, the electric current solution can be obtained using the voltage equation, and using this electric current solution, the electromagnetic force can be determined. To obtain the displacement response of the voice coil for this electromagnetic force, the electromagnetic force waveform is, by FFT, decomposed into frequency components. In this way, the displacement response is obtained and compared with the initially assumed displacement. When these displacements do not converge, the electric current waveform and electromagnetic force are obtained again using the newly produced displacement, and the results are compared with a newly obtained displacement waveform. When the displacements converge, the exciting force at that time is regarded as the final exciting force and the sound pressure waveform at the sound-receiving point is produced for the exciting force.

2.3 Analysis of electromagnetic system

To obtain the magnetic flux density, inductance and speedance, an electromagnetic analysis was carried out using FEM. Fig. 3 shows the boundary conditions and modeling shape of the magnetic circuit. Since the magnetic circuit was round, 2-dimensional modeling was conducted for the given axis-direction conditions. As for the remaining boundary conditions excepting the central axis, the magnetic vector potential was set at zero. Table 1 shows the material properties of the magnetic circuit. The yoke and top plate have a non-linear investment curve, and therefore a non-linear analysis using the

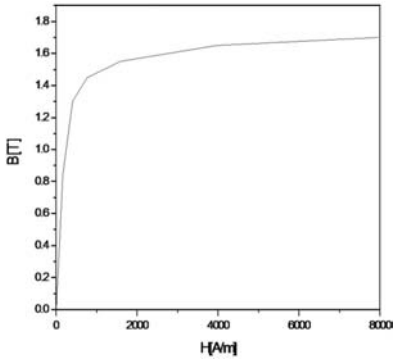

Fig. 4. B-H curve of yoke and top plate.

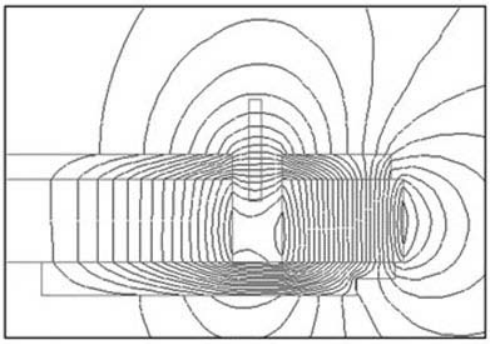

Fig. 5. Flux lines of magnetic circuit.

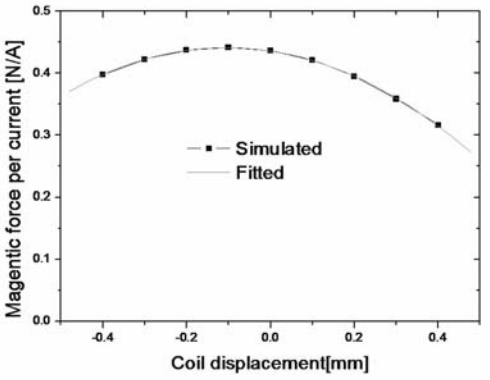

Fig. 6. Flux density for voice coil displacement.

B-H curve was performed. Fig. 5 graphically depicts the magnetic flux lines obtained through the analysis. The magnetic circuit of a microspeaker is thin, and therefore, when the voice coil moves up and down, the magnetic flux density interlinking with the voice coil varies. This average magnetic flux density can be obtained by

$$B_m = \frac{\int B_r dV}{V} \tag{1}$$

where B_r and V are the radial flux density and the volume of the voice coil, respectively. Fig. 6 plots the average magnetic flux density as a function of the voice coil displacement. When represented in the form of a quadratic function for the

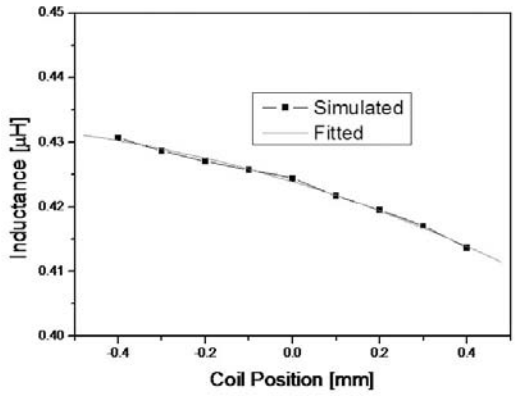

Fig. 7. Inductance along the displacement of coil.

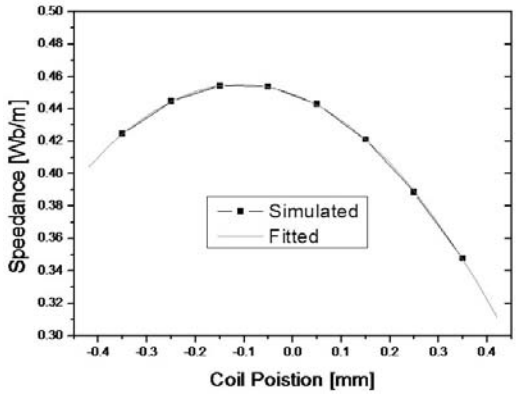

Fig. 8. Inductance along displacement of coil.

purposes of a coupling analyasis, the average magnetic flux density is

$$B_m(z) = 0.2 + 0.2z + 0.2z^2 \tag{2}$$

where z is the voice coil displacement. According to Faraday's law, the variance in the magnetic field with time generates an electric field. And as the flux linkage in the voice coil changes with time, a back electromotive force is generated in the voice coil, which can be summarized as

$$e = \frac{d\lambda}{dt} = \frac{d\lambda}{dI}\frac{dI}{dt} + \frac{d\lambda}{dz}\frac{dz}{dt} \tag{3}$$

The variance of the flux linkage with the electric currents is called inductance, and the variance with the coil position change is called speedance.

Using the flux linkage within the coil, which can be obtained by

$$\lambda = n\int B_z dV \tag{4}$$

the inductance and speedance according to the coil position can be analytically obtained. The results, plotted in Figs. 7 and 8, can also be represented as quadratic functions, as shown in expressions (5) and (6) below.

Table 2. Material properties of mechanical system.

Diaphragm	Density	1260 [kg/㎥]
	Young's modulus	6 [GPa]
	Thickness	25 [μ m]
Voice coil	Density	5910 [kg/㎥]
	Young's modulus	110 [GPa]
Air	Density	1.21 [kg/m^3]
	Sound velocity	341 [m/s]

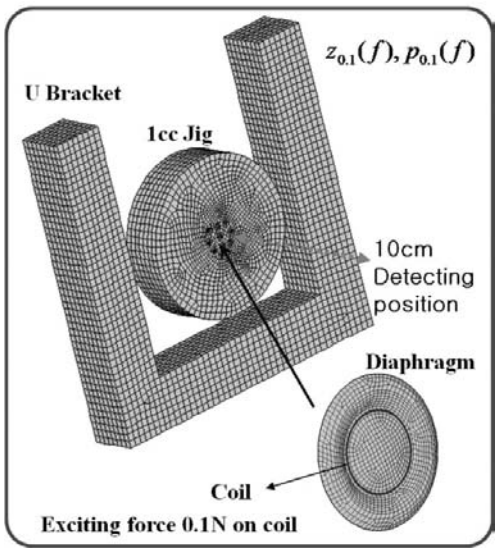

Fig. 9. Modeling of mechanical analysis.

$$L(z) = 0.2 + 0.2z + 0.2z^2 \tag{5}$$

$$K_e(z) = 0.2 + 0.2z + 0.2z^2 \tag{6}$$

2.4 Analysis of mechanical system

In ans analysis of the mechanical vibration system, the displacement and sound pressure of the voice coil were obtained for the exciting force of 0.1N. The commercial software Sysnoise was used in the analysis. Sysnoise has a function that can couple and solve structural FEM and acoustic BEM at the same time.

A structure consisting of the diaphragm and voice coil for FEM problem and a wall surface composed of a jig and a frame for acoustic BEM problem was modeled. Fig. 9 shows the modeling used in the analysis. In consideration of the measuring conditions, a 1cc jig and a U bracket to fix the jig were modeled. An exciting force 0.1N was applied to the voice coil, and a harmonic analysis was performed for each frequency. Table 2 lists the material properties used in the analysis. Fig. 10 plots the amplitude and phase of the voice coil displacement as functions of frequency. The phase represents the phase difference of the displacement for the exciting force. The resonance point is about 1.5 kHz, at which time the phase changes abruptly. Fig. 11 indicates the size and phase of the sound pressure at the sound-receiving point 10 cm from the jig. The phase continues to change, owing to the fact that the arrival distance of 10 incurs a phase delay.

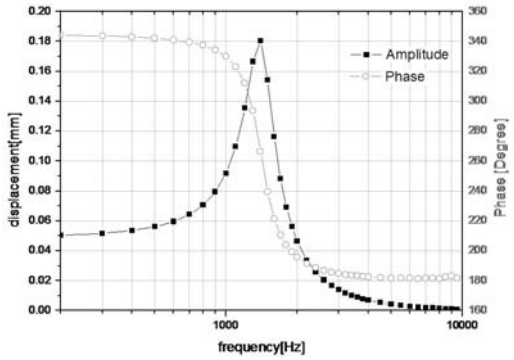

Fig. 10. Displacement of voice coil.

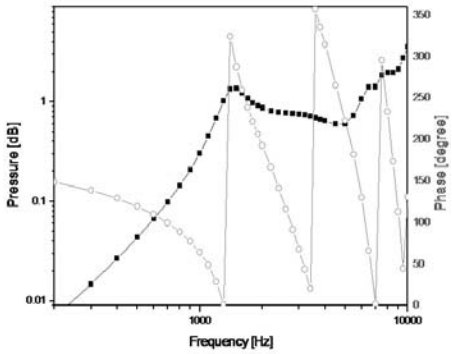

Fig. 11. Sound pressure at detection position.

2.5 Coupling analysis

A coupling analysis for each frequency was carried out as based on the previous analysis results. Once the frequency is determined, the initial vibration displacement can be assumed using the results of the vibration analysis, as shown in expression (7) below.

$$z(t) = z_0(f)\cos\{2\pi ft + \alpha(f)\} \tag{7}$$

Here, the displacement amplitude and phase difference are determined by the frequency. Using the supposed displacement, the magnetic flux density, inductance and speedance obtained in the electromagnetic system analysis can be converted to time functions. Then current waveforms can be obtained using the voltage equation.

$$V(t) = RI(t) + L(t)\frac{dI(t)}{dt} + K_e(t)\frac{dz(t)}{dt} \tag{8}$$

And, using the Lorentz force law, the sinusoidal exciting force generated in the voice coil can be obtained by expression (9) below.

$$F_{coil}(t) = B_m(t)I(t)l \tag{9}$$

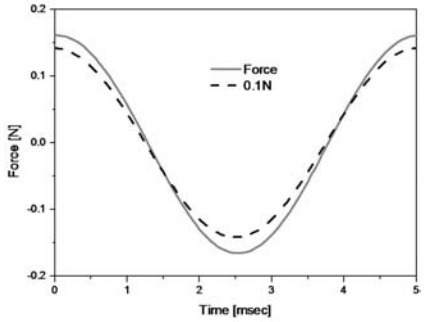

Fig. 12. Magnetic force on voice coil at 200 Hz.

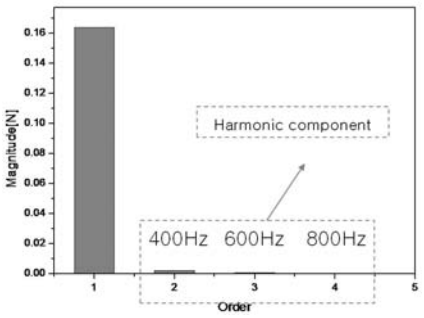

Fig. 13. Harmonic component of magnetic force at 200 Hz.

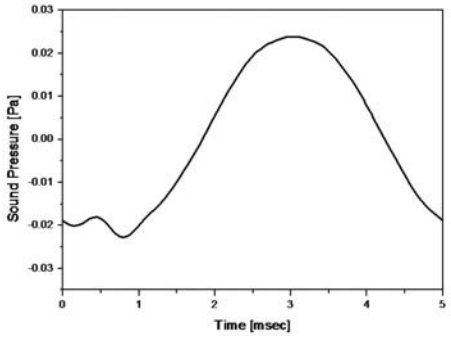

Fig. 14. Sound pressure at 200 Hz.

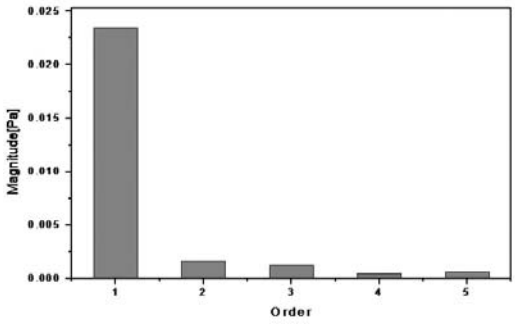

Fig. 15. Harmonic component of sound pressure at 200 Hz.

Fig. 12 plots the exciting force according to time at 200 Hz. When the exciting force is analyzed with FFT to obtain the displacement response it, the outcome can be expressed as in Fig. 13. It is found that an electromagnetic force that includes a harmonic component is generated for the input of the sinusoidal voltage signal. This is due to the change in the magnetic flux density with the movement of the voice coil. It is due also to the fact that electric current values, which are not linear to the input voltage, are generated as the speedance and inductance change. The amplitude of the displacement for the exciting force component with decomposed frequency can be represented by

$$z(t) = z_0 + \sum_n z_i(f_n)\frac{F_n}{0.1}\cos\{2\pi f_n t + \alpha_n(f_n) + \beta_n\} \tag{10}$$

A new displacement obtained by this expression is compared with the previously assumed displacement, and the error is derived. When the error deviates from the defined range, a new displacement is assumed as the initial displacement, and the electric current and electromagnetic forces are obtained. Then the actual new displacement is obtained. When the error falls within the defined range, the exciting force at that time is regarded as the final solution and the sound pressure at the sound-receiving point for the exciting force is obtained as shown in the following expression.

$$p(t) = \sum_n p_i(f_n)\frac{F_n}{0.1}\cos\{2\pi f_n t + \chi_n(f_n) + \delta_n\} \tag{11}$$

Fig. 14 shows the waveform of the sound pressure at the sound-receiving point. It can be seen that the waveform of the sound pressure for the sine wave is distorted significantly. The amplitude of the frequency component for this waveform is shown in Fig. 15. The high-order components of the sound pressure are more amplified than the those of the exciting force of the actual electromagnetic force. This is because the sound pressure responses of 400 Hz and 600 Hz, the high-order components of 200 Hz, are high.

In other words, higher-order sound pressure responses can appear at low frequencies even when there are only small electromagnetic force distortion components. The SPL and THD can be obtained for the above frequencies as follows.

$$SPL = 20\log(\frac{P_{rms}}{20\times10^{-6}}) \tag{12}$$

$$THD = \frac{\sqrt{\sum_{n=2} p_n^{\,2}}}{p_1} \tag{13}$$

At 200Hz, the SPL has a value of 53 dB and the THD has a value of 15%. In this way, the SPL and THD can be obtained for each frequency, as shown in Fig. 16. Overall, the THD is high in the low-frequency range because, as mentioned before, small high-order components can have the sound pressure responses of higher order components in the low-frequency band. Also, the magnetic system distortion is significant because the vibration displacement is relatively large.

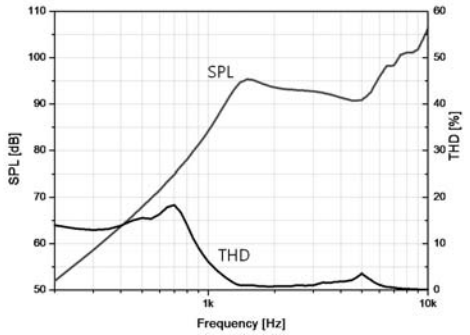

Fig. 16. SPL and THD for each frequency.

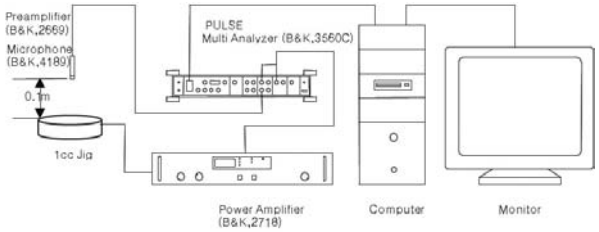

Fig. 17. Experimental setup.

2.6 Confirmatory experimentation

Fig. 17 shows the experimental setup for measurement of the sound pressure of a microspeaker. The B&K Pulse System (3560C), equipment exclusively used as an audio analyzer, was employed in the measurement. The signals of the audible area were regenerated into sweep noises in the pulse system and, subsequently, were amplified in the power amplifier.

The amplified signals were then regenerated in the microspeaker installed in the 1cc jig. As shown in Fig. 17, the input was received in a microphone positioned 10cm away, and was analyzed by FFT in the pulse system before being plotted as SPL and THD graphs. Fig. 18 shows a comparison between the simulated results and the experimental data. As is apparnet, the simulated results are in good agreement with the experimental data. As already mentioned, the SPL was low prior to the resonance point and, due to this, the THD was high. Overall, the THD in the low-frequency range was higher than that in the high-frequency range because the displacement in the low-frequency range was relatively large, and thus the electromagnetic distortion was large. Moreover, the THD was higher also because the high-order components were located near the resonance frequency, the sound response therefore having been large compared with the basic frequency. In the graph, there are some errors in the simulated versus experimental data as plotted. Above all, there is a difference in the sound pressure near the high-frequency range, which can be seen as the amplitude of the error for the amplitude of the factors when the FEM and BEM are used. Also, the THD shows some differences in the low-frequency range, which can be attributed to the fact that the present work examined

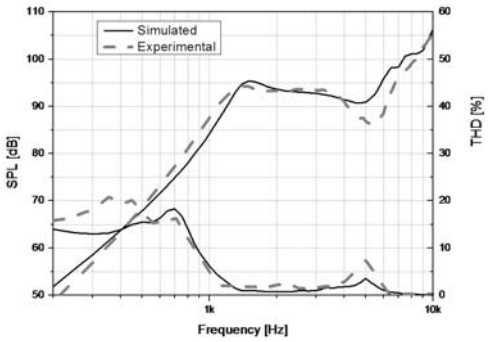

Fig. 18. Comparison between simulated results and experimental data.

the extent to which high-order components generated in the magnetic fields are influenced (or amplified or decreased) by the linearity of the vibration sound system: thus, the nonlinear characteristics of the vibration sound system were not considered.

3. Conclusions

Total harmonic distortion (THD) is a design factor central to high sound quality. In the present work, THD was analyzed in consideration of the magnetic and mechanical coupling effects. Simulated THD results were compared with the experimental data obtained. The results show that the THD in the lower frequency range was increased due to the displacement of the voice coil and the elevated mechanical responses of the high-order frequencies. It can be concluded therefore that low frequency THD in microspeakers can effectively by predicted using analytical approach here derived.

Acknowledgment

This work was financially supported by the Ministry of Education and Human Resources Development (MOE), the Ministry of Commerce, Industry and Energy (MOCIE) and the Ministry of Labor (MOLAB) through the fostering project of the Industrial-Academic Cooperation Centered University.

References

[1] S. M. Hwang, K. S. Hong, H. J. Lee, J. H. Kim and S. K. Jeung, Reduction of harmonic distortion in dual magnet type microspeaker, *IEEE Transactions on Magnetics*, 40 (4), (2004) .

[2] G. Y. Hwang, H. G. Kim, S. M. Hwang, and B. S. Kang, Analysis of harmonic distortion due to uneven magnetic filed in microspeaker used for mobile phones, *IEEE Transaction on Magnetics*, 38 (5) (2002).

[3] G. H. Jang and D. K. Lieu, The Effect of Magnetic Geometry on Electric Motor Vibrations, *IEEE Transactions On Magnetics*, 27 (1991).

[4] L. E. Kinsler, *Fundamentals of Acoustics* : Wiley, (1982).

[5] F. F. Mazda, *Electronic Instruments and Measurement*

Techniques. Cambridge Univ. Press, Cambridge, U. K., (1987).

Lee Chang-Min received his B.S. degree in Mechanical Engineering from Pusan National University, Korea, in 2010. He is now studying in the doctoral program at the same institution. His main research interest is THD reduction in microspeakers.

Hwang Sang-Moon received his B.S. degree in Mechanical Engineering from the University of California at Berkeley, USA, in 1990, and his Ph.D. in 1994. Currently he is a professor of Mechanical Engineering at Pusan National University, Korea. He is also CTO of Em-Tech, a Korean microspeaker company. His primary research interest is new magnetic circuits in microspeakers.